Cruickshank, W. H., and Kaplan, H. (1975), *Biochem. J. 147,* 411–416.
Cruickshank, W. H., Radhakrishnan, T. M., and Kaplan, H. (1971), *Can. J. Biochem. 49,* 1225–1232.
Dayhoff, M. O. (1972), Altas of Protein Sequence and Structure, Washington, D.C., National Biomedical Research Foundation.
Henkart, P. (1971), *J. Biol. Chem. 246,* 2711–2713.
Hill, R. J., and Davies, R. W. (1967), *J. Biol. Chem. 242,* 2005–2012.
Hirs, C. H. W., Halmann, M., and Kycia, J. H. (1965), *Arch. Biochem. Biophys. 111,* 209–222.
Hunkapiller, M. W., Smallcombe, S. H., Whitaker, D. R., and Richards, J. H. (1973), *Biochemistry 12,* 4732–4743.
Imoto, T., Johnson, L. N., North, A. C. T., Phillips, D. C., and Rupley, J. A. (1972), *Enzymes, 3rd Ed., 7,* 665–868.
Kaplan, H. (1972), *J. Mol. Biol. 72,* 153–162.
Kaplan, H., and Dugas, H. (1969), *Biochem. Biophys. Res. Commun. 34,* 681–685.
Kaplan, H., and Duggleby, R. G. (1975), *Canadian Federation of Biological Societies,* Winnipeg.
Kaplan, H., Stevenson, K. J., and Hartley, B. S. (1971), *Biochem. J. 124,* 289–299.
Mares-Guia, M., and Shaw, E. (1965), *J. Biol. Chem. 240,* 1579–1585.
Matthews, B. W., Sigler, P. B., Henderson, R., and Blow, D. M. (1967), *Nature (London) 214,* 652–656.
Meadows, D. H., Markley, J. L., Cohen, J. S., and Jardetzky, O. (1967), *Proc. Natl. Acad. Sci. U.S.A. 58,* 1307–1313.
Murdock, A. L., Grist, K. L., and Hirs, C. H. W. (1966), *Arch. Biochem. Biophys. 114,* 375–390.
Olafson, R. W., Jurášek, L., Carpenter, M. R., and Smillie, L. B. (1975), *Biochemistry 14,* 1168–1177.
Olafson, R. W., and Smillie, L. B. (1975), *Biochemistry 14,* 1161–1167.
Olson, M. O. J., Nagabhushan, N., Dzwiniel, M., Smillie, L. B., and Whitaker, D. R. (1970), *Nature (London) 228,* 438–442.
Robillard, G., and Shulman, R. G. (1974), *J. Mol. Biol. 86,* 519–540.
Shotton, D. M., and Watson, H. C. (1970), *Nature (London) 225,* 811–816.
Sigler, P. B., Blow, D. M., Matthews, B. W., and Henderson, R. (1968), *J. Mol. Biol. 35,* 143–164.
Valenzuela, P., and Bender, M. L. (1969), *Proc. Natl. Acad. Sci. U.S.A. 63,* 1214–1221.
Valenzuela, P., and Bender, M. L. (1970), *Biochemistry 9,* 2440–2446.
Visentin, L. P., Yaguchi, M., and Kaplan, H. (1973), *Can. J. Biochem. 51,* 1487–1497.

Molecular Mobility and Structure of Elastin Deduced from the Solvent and Temperature Dependence of ^{13}C Magnetic Resonance Relaxation Data†

J. R. Lyerla, Jr.,‡ and D. A. Torchia*

ABSTRACT: ^{13}C relaxation parameters, T_1, line width, and NOE, have been determined for backbone carbons of ligamentum nuchae elastin swollen by 0.15 *M* NaCl, 0.15 *M* NaCl–formamide, 0.15 *M* NaCl–ethanol, dimethyl sulfoxide, and formamide. The data have been analyzed in terms of (a) a single correlation time model and (b) a model employing a log-χ^2 distribution of correlation times used by Schaefer (1973) to analyze solid *cis*-polyisoprene ^{13}C relaxation data. Employing the latter mode, one obtains an approximately self-consistent quantitative analysis of all the elastin data. An average backbone correlation time, $\bar{\tau}$, of ca. 2 nsec is calculated for elastin swollen in the presence of polar organic solvents at 37°, in approximate agreement with $\bar{\tau}$ of 0.4 nsec obtained for bulk *cis*-polyisoprene at 35°. The influence of solvent and temperature on elastin spectra indicate that the larger $\bar{\tau}$ value (~80 nsec) obtained for elastin swollen by 0.15 *M* NaCl at 37° is a consequence of weak interchain polar and hydrophobic interactions, a result which is in accord with the reported viscoelastic behavior exhibited by water-swollen elastin at 37°. The results obtained further suggest that Gly, Pro, and Val residues are significantly more mobile than Ala residues, which are located in the cross-link regions. Hence, the NMR data support the view that water-swollen elastin is composed of a network of mobile chains, except possibly in the cross-link regions.

Elastin is an important component of connective tissues such as skin, lung, blood vessel, and ligament. Tissues containing elastin fibers have the useful (rubber-like) mechanical properties of high elasticity and small elastic modulus. In view of the similar mechanical properties of elastin fibers and natural rubber, a fundamental question is: does the elasticity of these two materials arise from common structural features at the molecular level?

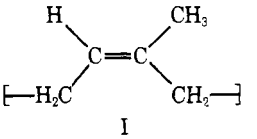

I

† From the Laboratory of Biochemistry, National Institute of Dental Research, Bethesda, Maryland 20014. *Received August 12, 1975.*
‡ Present address: IBM Corporation, Department K42/282, San Jose, California 95193.

Natural rubber consists of long chains of *cis*-isoprene units (I). Due to the weak intermolecular forces between the nonpolar isoprene units, the chains are kinetically free (at room temperature) and in the relaxed state they adopt a Gaussian distribution of lengths. When rubber is stretched, the chains are constrained to extend in the direction of the applied stress, resulting in a decrease in their conformational entropy which produces the elastic restoring force (Flory, 1953; Treloar, 1958). The introduction of interchain cross-links creates a three-dimensional network which prevents stress induced plastic flow.

At the molecular level, elastin has structural features in common with rubber. First, (soluble) proelastin chains are long polypeptides (mol wt ~70000) (Sandberg et al., 1969; Smith et al., 1972) containing about 850 peptide units (II).

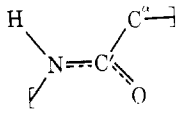

II

Second, the individual polypeptide chains are cross-linked (by desmosine and isodesmosine) to form elastin fibers (Thomas et al., 1963).

One major difference in the properties of elastin fibers and rubber is that the former must be swollen by water (or another highly polar solvent) to exhibit elasticity. Dried elastin fibers are brittle and glass-like. This difference in behavior between unswollen elastin fibers and rubber is due to the fact that, unlike rubber, elastin contains polar NH and C′O moieties. The strong interactions between these polar moieties in the polypeptide backbone prevent kinetic freedom of elastin chains in dry fibers at room temperature.

The fact that the swelling of elastin in water depends upon temperature and stress complicates the analysis of thermoelastic and mechanical data (Hoeve and Flory, 1958; Oplatka et al., 1960) and has caused much of the controversy surrounding the interpretation of such data. The earliest thermoelastic studies of elastin (Meyer and Ferri, 1936; Wohlisch et al., 1943) were interpreted as showing that the behavior of elastin fibers deviated significantly from that of natural rubber. Hoeve and Flory (1958) pointed out that these conclusions were unwarranted since the deswelling of water-swollen elastin with elevation of temperature had been neglected in the data analyses. Hoeve and Flory (1958) further concluded that the thermoelastic properties of elastin were indeed those of an ideal rubber when the protein was swollen in water–ethylene glycol, 7:3, v/v, a solvent system in which the elastin volume is independent of temperature.

The analysis of Hoeve and Flory (1958) was itself criticized by several groups of investigators (Oplatka et al., 1960; Hoffman, 1971; Weis-Fogh and Andersen, 1970a,b; Mistrali et al., 1971). Although Mistrali et al. (1971) concluded that their data supported the network model, alternative models of elastin structure were proposed as additional data on elastin chemistry and physical properties accumulated. Partridge (1970) suggested a two-phase globular model for elastin swollen in water. In the Partridge model, the polypeptide chains, which are known to be ca. 95% nonpolar (Partridge, 1962; Gray et al., 1973), are supposed to pack into spherical globules (diameter ca. 50 Å) so as to minimize the contacts between hydrophobic side chains and the water phase, which surrounds, but does not penetrate the globules. Weis-Fogh and Andersen (1970a,b) concluded that their calorimetric measurements on elastin ruled out the network model but did support the globular model. These investigators proposed that the retractive force of elastin fibers was due to a decrease in water entropy, which they suggested occurs because stretching causes an increase in the area of interfacial contact between the water and the hydrophobic globules. An alternative model of elastin structure which invokes hydrophobic interactions to account for elasticity is the "oiled-coil" model recently formulated by Gray et al. (1973). In this model, helical rather than globular conformations are assumed for the polypeptide chains on the basis of regularities in the proelastin sequence. In common with the other two-phase models, chain mobility is severely restricted in the "oiled-coil" model since preferred conformations are present in both relaxed and stretched fibers.

At present the nature of elastin's structure is still actively debated. Hoeve and Flory (1974) and Grut and McCrum (1975) have pointed out that the network model is consistent with the thermoelastic data of Weis-Fogh and Andersen (1970a,b) when the increased swelling, caused by stress, is considered in the analysis. While these investigators agree that the rubber-like network model accounts for the properties of elastin at equilibrium, Dorrington et al. (1975) have suggested that, at 37°, the water swollen elastin network is viscoelastic (i.e., like natural rubber at low temperature) to account for their dynamical-mechanical measurements. In contrast, Mukherjee et al. (1974) claim that their viscoelastic data support the two-phase "oiled-coil" model of Gray et al. (1973).

Since the compact chains in the two-phase models of elastin are expected to be much less mobile than the random coil chains in a rubber-like network, information on the mobility of elastin chains is useful for distinguishing between the two types of models. From measurements of ^{13}C relaxation times of elastin carbonyl carbons in water swollen calf ligamentum nuchae, Torchia and Piez (1973) found that ca. 80% of the elastin backbone carbonyl carbons undergo rapid segmental motion characterized by an average rotational correlation time of ca. 40 nsec. Although this result supports the rubber-like network rather than the two-phase models, the spin-lattice relaxation time was the only nuclear magnetic resonance (NMR) parameter determined, and the corresponding correlation time was obtained assuming a simple model of elastin segmental motion: namely, that rotational reorientation of backbone carbons is isotropic and characterized by a single correlation time. Schaefer (1973) has shown that NMR parameters T_1, Δ,[1] and NOE of bulk rubber-like polymers are better interpreted using a distribution of correlation times rather than the single correlation time model. In view of this result and the known strong influence of solvent and temperature on elastin's properties, we have determined the NMR relaxation pa-

[1] Abbreviations used are: FID, free induction decay; H_o, the external magnetic field; T_1, the ^{13}C spin-lattice relaxation time; Δ, the full line width at half-peak height; NOE, the ^{13}C-$\{^1H\}$ nuclear Overhauser enhancement; N, the number of protons directly bonded to a protonated carbon; τ_R, the correlation time in the single correlation time model; $\bar{\tau}$, the correlation time which defines the approximate maximum of the log-χ^2 distribution; τ' is the most probable correlation time and equals $\bar{\tau}(p-1)/p$; $\langle\tau\rangle$ is the mean correlation time and equals $\bar{\tau}\{[1 - \ln(b)/p]^{-p} - 1\}/(b-1)$ when $p > \ln b$; b, the base used to define the log-χ^2 distribution; p, the number of degrees of freedom of the log-χ^2 distribution; ϵ, the dielectric constant.

rameters as a function of solvent and temperature. These data have been analyzed using a single correlation time as well as a distribution of correlation times, and the new information on elastin mobility so obtained is used to evaluate the current models of elastin structure.

Experimental Section

Sample Preparation and Analysis. Ligamentum nuchae, obtained from a 6-week-old calf, was washed several times with a 0.15 *M* NaCl solution to remove blood and soluble matter. Samples of ligament were then scraped free of extraneous matter, coarsely cut, and washed several times with deionized water. Pieces of ligamentum nuchae were then immersed in the appropriate solvent, and, after several solvent exchanges, the ligament was allowed to remain in contact with the swelling agent for ca. 1 day (at room temperature). The swollen sample was then packed into the 10-mm NMR tube to a height of 22 mm (sample volume, 1.4 ml) to ensure that the entire sample was within the volume of the transmitter–receiver coil of the probe.

Collagen was removed from some samples of ligament using the procedure of Partridge et al. (1955). The ligamentum nuchae sample was autoclaved in water four times at a pressure of 1 atm for ca. 40 min. After soaking the ligament several times in a 1:1 v/v mixture of diethyl ether–ethanol, specimens were soaked in ethanol and then in deionized water. Samples were swollen in the appropriate solvents and prepared for NMR work in the manner described above.

After completion of the NMR experiments, each specimen of ligament was soaked (several times) in large volumes of distilled water. These water-swollen samples were then dried under vacuum for 48 hr and weighed immediately. A small portion of each dried sample (1–3 mg) was hydrolyzed in 6 *N* HCl at 110° for 28 hr and then subjected to quantitative amino acid analysis. The autoclaved sample had the elastin composition reported by Gotte et al. (1963), while the native samples were found to contain about 15% collagen by weight. The analyses further showed that the NMR sample tube typically contained about 200–300 mg of elastin.

Samples of achilles tendon collagen were also obtained from the 6-week-old calf and were prepared for NMR work in the manner described for native ligamentum nuchae.

^{13}C Fourier Transform Spectra. The 15.08-MHz ^{13}C "home-built" spectrometer described previously (Farrar et al., 1972; Torchia and Lyerla, 1974; Torchia et al., 1975) was used to obtain all spectra. Constant sample temperature was maintained in the Dewared probe using a Varian temperature controller. The pulse power delivered to the single coil probe was sufficient to rotate the ^{13}C magnetization by 90° in 2.5 μsec. The proton decoupler was gated using a unit designed and built by Dr. D. L. VanderHart of the National Bureau of Standards.

All samples were confined to a volume (1.4 ml) within the transmitter–receiver coil using 10-mm Teflon vortex plugs. Oxygen was not removed from the samples since all T_1 values were less than 1.5 sec. Approximately 1–5 μl of acetonitrile, 90% ^{13}C enriched at the methyl carbon, was added to most samples, and the methyl resonance (191.7 ppm, relative to external CS_2) served as an internal reference. The shape and width of the acetonitrile resonance served as sensitive monitors of the magnetic field homogeneity and stability during data accumulation.

Data Acquisition. Free induction decays (FID) were accumulated in a Nicolet 1080 data system using spectral windows of 7813 Hz. Digital resolution of transformed spectra was 4 Hz/channel. The accumulated FID were digitally filtered to improve the signal to noise ratio at the expense of either 5 or 10 Hz added line width. Nicolet software programs were used to phase correct the transformed spectra and to obtain integrated intensities.

Determination of NMR Relaxation Parameters. Carbonyl spin–lattice relaxation times were calculated from integrated intensities of resonances in inversion–recovery spectra (Vold et al., 1968; Allerhand et al., 1971) as described by Torchia and Lyerla (1974). NOE values were determined (using 90°-t-90° pulse sequences with t at least three times greater than the largest T_1) from a comparison of spectra obtained using (a) continuous broad band decoupling and (b) gated broad band decoupling with the 60 MHz transmitter gated on only during acquisition of the FID. The gated spectrum was multiplied by a scale factor and then subtracted (in the 1080 computer) from the continuously decoupled spectrum. The scale factor which yielded a nulled difference spectrum for a given resonance (or group of resonances) was taken as the NOE value for the resonance. Line widths of protonated carbons were estimated using a computer simulation technique described previously (Torchia et al., 1975). As input, the simulation program required the intensity, chemical shift, and line width of each carbon in elastin. The intensities (appropriate to the gated spectra, i.e., no NOE) were obtained from the ligamentum nuchae amino acid analyses (see above). Chemical shifts of elastin carbons were obtained from ^{13}C data of polypeptides having sequences similar to the sequence of elastin (Gray et al., 1973; Urry et al., 1974; Torchia et al., 1975). Initial values of elastin line widths were estimated by inspection of the experimental spectrum and were then varied until a satisfactory stimulation (Figure 6) was obtained. The values listed in Table II do not include the 10-Hz instrumental contribution to the line width.

Correlation Time Calculations. The curves (Figure 1) relating the NMR parameters and the protonated carbon (single) correlation time, τ_R, were calculated using standard formulas (Solomon, 1955; Abragam, 1961; Doddrell et al., 1972; Schaefer and Natusch, 1972). Although peptide carbonyl carbons are not protonated, $^{13}C'$–H dipolar interactions are almost entirely responsible for relaxation of polypeptide C′ spins when H_0 = 14 kG (Torchia and Lyerla, 1974; Torchia et al., 1975). We are unable to make an exact calculation of the dependence of T_1 and T_2 ($T_2^{-1} = \pi\Delta$) on τ_R since the distance between the C′ carbon and some of the protons which contribute to the C′ relaxation process depends upon the polypeptide conformation. An approximate calculation, similar to that of Torchia and Lyerla (1974), predicts that C′ T_1 and T_2 values (averaged over the residues in elastin) are about 20 times those of a C^α (methine) carbon having the same τ value. In fact, polypeptide data (Torchia and Lyerla, 1974; Torchia et al., 1975) show that C′ T_1 values in a given polypeptide are about 15 times C^α NT_1 values (N is the number of protons bonded to C^α) and the empirical relationship $T_1(C') = 15NT_1(C^\alpha)$; $\Delta(C') = \Delta(C^\alpha)/15N$ was used to obtain the C′ curves in Figure 1.

The calculations were extended to include a distribution of correlation times by replacing the single correlation time appearing in the spectral density equations of Solomon (1955) by a log-χ^2 distribution of correlation times as described by Schaefer (1973).

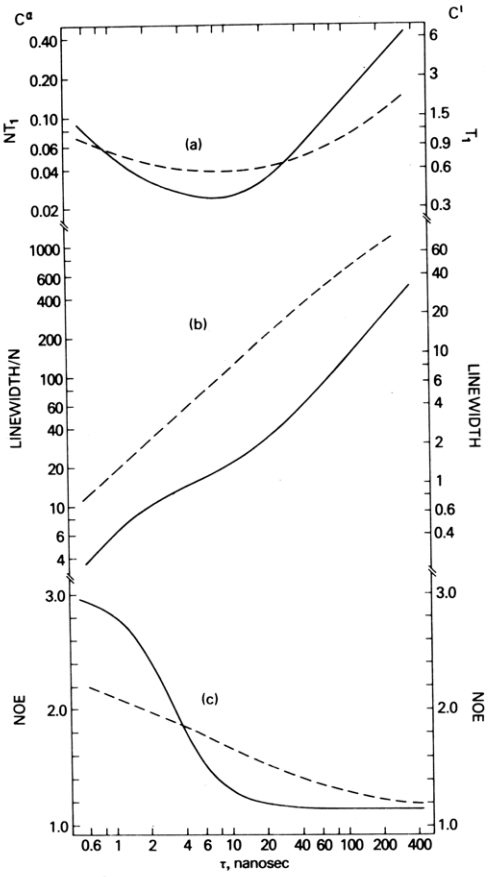

FIGURE 1: NMR parameters at H_o = 14 kG: (a) T_1; (b) $\Delta = 1/(\pi T_2)$; (c) NOE; plotted (1) as a function of $\tau = \tau_R$ in the single correlation time model (solid curves) and (2) as a function of $\tau = \bar{\tau}$ in the log-χ^2 distribution of correlation times model having b = 1000, p = 14 (dashed curves). The log-χ^2 distribution and the parameters p, b, and $\bar{\tau}$ are defined in eq 1 and 2. The scales on the left apply to a C^α carbon, dipolar relaxed by the N hydrogens to which it is bonded, with r_{CH} = 1.09 Å. The scale on the right applies to a C′ carbon, dipolar relaxed by proximal protons (see Experimental Section for further explanation of C′ calculation).

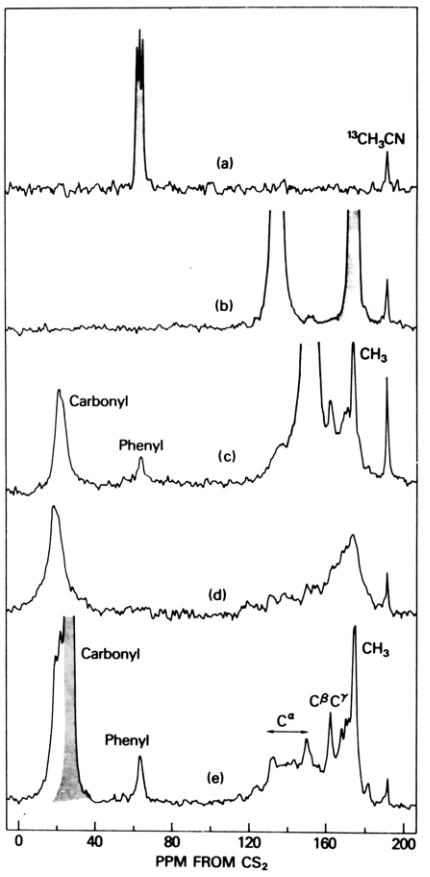

FIGURE 2: Comparison of calf ligamentum nuchae spectra obtained in five solvents at 37°, using 90°-t-90° pulse sequences: (a) benzene-d_6, t = 1.0 sec; (b) ethanol, t = 1.0 sec; (c) dimethyl sulfoxide, t = 3.2 sec; (d) 0.15 M NaCl, t = 3.5 sec; (e) formamide, t = 1.0 sec. 4K transients accumulated in (a), 8K transients accumulated in (b–d). Chemical shift scale in ppm from external CS_2. Solvent resonances are shaded.

Results and Discussion

In order to relate the measured parameters T_1, Δ, and NOE to molecular mobility, one must know the mechansim responsible for the ^{13}C spin relaxation and assume a model for molecular motion. In the case of polypeptides, it has been established that (when H_o = 14 kG) the ^{13}C-$\{^1H\}$ dipole–dipole interaction is responsible for relaxation of protonated and carbonyl carbons (Torchia and Lyerla, 1974; Torchia et al., 1975). The simplest model for the motion of internuclear C–H vectors assumes that rotational reorientation is isotropic and is characterized by a single correlation time, τ_R, equal to $1/(6R)$, where R is the diffusion coefficient for the C–H rotational motion. In the case of isotropic reorientation, theoretical expressions relating the NMR parameters and τ_R are available (Solomon, 1955; Doddrell et al., 1972). The plots of T_1, Δ, and NOE vs. τ_R (solid curves in Figure 1) illustrate the results of the theory applied to protonated and C′ carbons. Initially, the simple isotropic model is used to analyze the data; however, it will be seen that a more complex model, involving a distribution of correlation times (Connor, 1963; Schaefer, 1973), is required for a satisfactory quantitative analysis of the data.

Before discussing the experimental data it is worth emphasizing that ^{13}C resonances will not be detected (using the high-resolution technique employed herein) unless chain flexibility is sufficient to reorient rapidly internuclear C–H vectors over essentially all solid angle. For instance, the solid curves in Figure 1 show that if $\tau_R > 50$ nsec, then T_1 and Δ increase linearly as τ_R increases. When $\tau_R = 1$ μsec, $\Delta > 10^3$ Hz for protonated carbons while $T_1 > 25$ sec for C′ carbons. Hence, if $\tau_R > 1$ μsec, protonated carbon resonances will be too broad to detect while the time required to accumulate C′ signals will exceed practical limits. Since line widths increase monotonically as molecular mobility decreases (Figure 2b), the breadths of elastin resonances in a given solvent provide a qualitative indication of chain mobility. It is clear from the ^{13}C spectra of calf ligamentum nuchae in Figure 2 that elastin line widths, and hence flexibility, are markedly dependent on solvent polarity. An elastin spectrum is not obtained in the solvents of lowest dielectric constant, i.e., benzene-d_6 (ϵ 2) and ethanol (ϵ 24)—indicating that ^{13}C C^α resonance lines are broader ($\Delta > 10^3$ Hz) than the detection limits of the high-resolution techniques employed here. In contrast, line widths for α-backbone carbons are of the order of 50 Hz in the highly polar organic solvents dimethyl sulfoxide (ϵ 45) and formamide (ϵ 110). Apparently, intermolecular polar interactions between elastin chains are reduced in aqueous 0.15 M NaCl, dimethyl sulfoxide, and formamide to the extent that elastin chains have $\tau_R < 1$ μsec.

Comparison of spectra in the three polar solvents (Figure 2c–e) shows that resonance lines are sharper in dimethyl

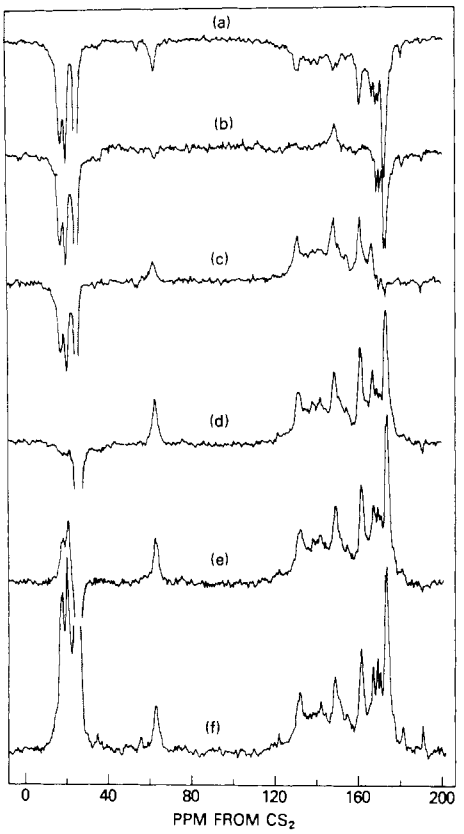

FIGURE 3: Representative partially relaxed spectra of calf ligamentum nuchae swollen in 0.15 *M* NaCl-formamide, 5:4 by volume, at 37° obtained using 180°-*t*-90° pulse sequences with (a) t = 0.010 sec; (b) t = 0.040 sec; (c) t = 0.10 sec; (d) t = 0.40 sec; (e) t = 0.75 sec; (f) a 90°-*t*-90° spectrum. The recovery time following the 90° pulse was 1.0 sec in (a-c) and 5.0 sec in (d-f). 8K or 12K transients were accumulated in each case and the intensities have been normalized. The chemical shift scale is in ppm from external CS_2 and the solvent resonance is shaded in each spectrum.

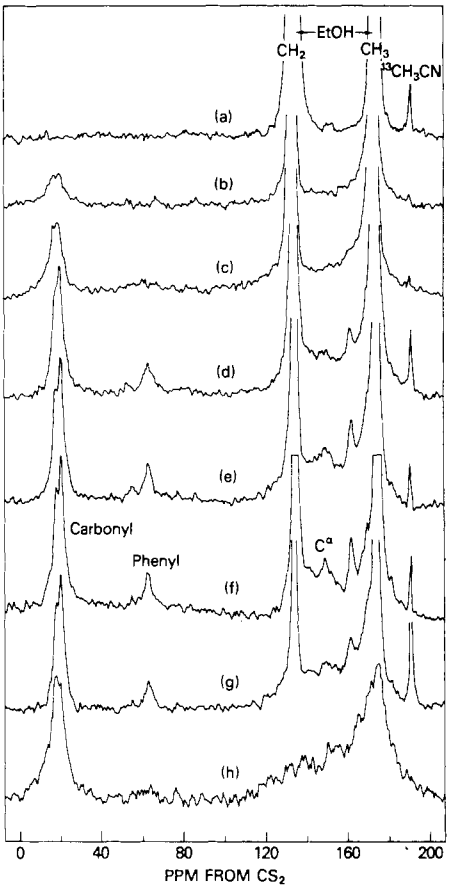

FIGURE 4: Spectra of calf ligamentum nuchae at 37° showing the dependence of the line widths on the aqueous volume fraction, A_f, in 0.15 *M* NaCl-ethanol solvent mixtures: (a) A_f = 0.0; (b) A_f = 0.06; (c) A_f = 0.11; (d) A_f = 0.20; (e) A_f = 0.33; (f) A_f = 0.50; (g) A_f = 0.67; (h) A_f = 1.0. In each case, 8K transients were accumulated using 90°-*t*-90° pulse sequences with t = 1.0 sec. Chemical shift scale in ppm from external CS_2. The spectral changes were reversible.

sulfoxide and formamide than 0.15 *M* NaCl. For instance, the Phe ring carbon resonances are resolved in the polar organic solvents but not in 0.15 *M* NaCl. The greatest fine structure is evident in the formamide spectrum where resonances corresponding to methyl carbons of Leu (172-173 ppm), Val (175 ppm), Ala (176-178 ppm), and Ile (182 ppm) are identifiable. A well-resolved ^{13}C spectrum of elastin at 37° was also found in a mixed solvent system, 0.15 *M* NaCl-formamide, 5:4, v/v (Figure 3f). In addition, certain mixtures of 0.15 *M* NaCl-ethanol yielded elastin spectra (Figure 4) which were significantly sharper than found when either solvent was used alone—the smallest line width being obtained at a 1:1 volume ratio (Figure 4f). A quantitative discussion of elastin mobility and structure in a particular solvent requires the examination of the signal intensity, T_1, T_2, and NOE values to which we now turn.

Solvent resonances obscure much of the upfield region in certain elastin spectra, hence the intensities of the carbonyl resonances (16-22 ppm) of the various spectra are most readily compared. Since the integrated intensity of a high-resolution ^{13}C resonance (obtained under appropriate conditions; see Experimental Section) is proportional to the number of carbon nuclei which contribute to the resonance, the fraction of mobile ($\tau < 10^{-6}$ sec) carbonyl carbons in elastin can be determined from measured C′ resonance intensities. Previously, C′ intensity data, obtained for elastin swollen in 0.15 *M* NaCl, showed that ca. 80% of the backbone carbonyl carbons are mobile with τ_R ca. 40 nsec (Torchia and Piez, 1973). In the experiments described herein, the same sample volume (1.4 ml; see Experimental Section) was used to obtain each spectrum. Since the swelling of the ligament is solvent dependent, amino acid analysis was used to determine the weight of elastin in each sample. It is seen (Table I) that the C′ signal intensity per milligram of elastin is independent of solvent,[2] implying that ca. 80% of the elastin backbone carbons are mobile when ligamentum nuchae is swollen by any of the highly polar solvents used in this study.

Values of T_1, Δ, and NOE obtained for backbone car-

[2] Amino acid analysis showed that collagen constituted about 15% of the protein in the samples of ligamentum nuchae used in this work. When calf tendon is swollen by 0.15 *M* NaCl and 0.15 *M* NaCl-EtOH, 1:1, v/v, or dimethyl sulfoxide, the resonances of the rigid collagen molecules are not detectable. Hence, collagen does not contribute to the high-resolution spectra of ligamentum nuchae swollen in these solvents. However, spectra of collagen are obtained, at 37°, when calf tendon is swollen by the solvents containing formamide and the measured intensities indicate that about ⅓ of the tendon denatures (and contributes to the spectrum) in neat formamide and about ⅕ denatures in 0.15 *M* NaCl-formamide, 5:4 v/v. Hence, a small percentage (5-10%) of the ligament carbonyl intensity is due to denatured collagen in the formamide containing solvents. For this reason, collagen was removed from certain samples of ligament and the carbonyl intensity obtained from spectra of these samples was used to calculate the results presented in Table I.

Table I: Comparison of Elastin Carbonyl Intensity Data[a] Obtained in Various Solvents at 37°.

	Intensity[b]	Intensity/ Unit Mass	Percentage of Mobile Carbon[f]
0.15 *M* NaCl	100	518	80
0.15 *M* NaCl–EtOH[c]	91	442	70
0.15 *M* NaCl–formamide[d,e]	86	522	81
Dimethyl sulfoxide	53	550	86

[a] Spectra were obtained using gated decoupling to suppress the NOE. [b] Integrated intensities were normalized to compensate for differences in number of scans and software scaling factors. [c] 1:1, v/v. [d] 5:4, v/v. [e] Data obtained from spectra of collagen-free ligamentum nuchae. [f] Estimated uncertainty ±15%.

Table II: Comparison of Elastin T_1,[a] Δ,[b] and NOE[c] Values Obtained in Various Solvents at 37°.

	C′		Cα		
	T_1	NOE	NT_1	Δ/*N*	NOE
0.15 *M* NaCl–formamide[d]	0.7	1.9	60	40	2.0
0.15 *M* NaCl–ethanol[e]	0.75	1.9	60[f]	80[f]	2[f]
Dimethyl sulfoxide	0.7	1.8	60[g]	80[g]	2[g]
0.15 *M* NaCl	1.1	1.5		700	1.5

[a] In sec, uncertainty ±15%, unless otherwise noted. [b] In Hz, uncertainty ±20%, unless otherwise noted. [c] Uncertainty ±10%, unless otherwise noted. [d] 5:4, v/v. [e] 1:1, v/v. [f] Due to solvent interference, only the Gly Cα values were determined, uncertainty ±25%. [g] Due to solvent interference, only the Pro Cα values were determined, uncertainty ±25%.

bons of elastin, swollen in the various polar solvents, are listed in Table II.[3] The procedures which were used to obtain these parameters are described in the Experimental Section. In terms of the single correlation time model (Figure 1a, solid curve) the carbonyl and Cα T_1 values obtained in the presence of organic solvents (Table II) are in the region of the T_1 minimum and indicate that the backbone correlation time, in each case, is ca. either 1 or 40 nsec.

Since the line width and NOE values obtained in the presence of organic solvents are respectively smaller and larger than found in 0.15 *M* NaCl, the larger T_1 value obtained for C′ in 0.15 *M* NaCl (1.1 sec) corresponds to a τ_R value on the slow motion (right) side of the T_1 minimum, i.e., $\tau_R \sim 55$ nsec in 0.15 *M* NaCl. There is no ambiguity in calculating a correlation time from a line width or NOE value since these parameters are monotonic functions of τ_R (see Figure 1b,c). The backbone correlation times derived from the single correlation time model are listed in Table III. Examination of Table III shows that (a) the mobile backbone carbons in elastin are characterized by calculated rotational correlation times of less than 500 nsec in the four polar solvent systems and (b) τ_R is significantly larger in 0.15 *M* NaCl than in the solvents having an organic component. The evident internal inconsistency in the single correlation time analysis is that, in a given solvent, calculated τ_R values corresponding to the NMR parameters, T_1, Δ, or NOE, show variations of 1–2 orders of magnitude.

Table III: Comparison of Backbone Correlation Times,[a] τ_R, in Various Solvents as Derived from T_1, Δ, and NOE Values[b] and the Single Correlation Time Isotropic Model.[c]

Solvent	τ (T_1)	τ (Δ)	τ (NOE)
0.15 *M* NaCl–formamide[d]	1,40	30	4
0.15 *M* NaCl–ethanol[e]	1,40	60	4
Dimethyl sulfoxide	1,40	60	4
0.15 *M* NaCl	55	500	6

[a] In nsec. [b] See Table II. [c] See solid curves in Figure 1. [d] 5:4, v/v. [e] 1:1, v/v.

The failure of the single correlation time model to provide a satisfactory analysis of the elastin relaxation data is in accord with results of Schaefer (1973) who has shown that a broad distribution of correlation times must be assumed to account for ^{13}C relaxation data obtained for bulk rubbery polymers and viscous polymer solutions. A distribution of rotational correlation times has also been widely used to analyze dielectric and proton NMR data obtained in studies of molecular motion in bulk polymers (Connor, 1963). A distribution of correlation times is needed to describe polymer motion since the polymer is continually passing from one conformation to another and the local segmental motion is a function of the instantaneous conformation. Following Schaefer (1973), we assume a log–χ^2 distribution of correlation times:

$$G_p(s) = (ps)^{p-1}e^{-ps}p/\Gamma(p) \quad (1)$$

with

$$s = \log_b [1 + (b - 1)\tau/\bar{\tau}] \quad (2)$$

$G_p(s)ds$ is the probability of finding correlation time τ corresponding to $s = s(\tau)$. The width of the distribution is governed by the variables, p and b, and the use of a log $(\tau/\bar{\tau})$ argument in defining G allows very broad distributions to be employed. For $p \gg \ln b$ (a narrow distribution) $\bar{\tau}$, $\langle\tau\rangle$, and τ' are approximately equal, where $\langle\tau\rangle$ is the mean value of τ and τ' is the most probable value of τ. For broad distributions $\langle\tau\rangle > \bar{\tau} > \tau'$ (see footnote 1).

The NMR parameters, plotted as a function of $\tau(=\bar{\tau})$ in Figure 1 (dashed curves), were calculated assuming a distribution function having $p = 14$, $b = 1000$, which was used by Schaefer[4] (1973) to analyze the data obtained for *cis*-polyisoprene. The elastin $\bar{\tau}$ values calculated from each NMR parameter in the various solvents are given in Table IV.

As was true with the single correlation time model, each NMR parameter yields a different calculated value of $\bar{\tau}$ in a given solvent. However, the variation in $\bar{\tau}$ (Table IV) in a given solvent is less than a factor of five using the distribution of correlation time model. Because of the large uncertainties in the data, and the sensitive dependence of calculated values of $\bar{\tau}$ on measured values of T_1 and NOE, the

[3] The presence of collagen resonances in Figure 3 does not significantly affect the elastin T_1 values determined using these spectra for two reasons. First, collagen resonances account for less than 10% of the spectral intensity. Second, denatured collagen T_1 values (Torchia and Piez, 1973) differ by less than 20% from those obtained from Figure 3. The same NOE and Δ values were obtained for formamide swollen ligament samples containing and lacking collagen.

[4] In using eq 26 (Schaefer, 1973) to calculate the spectral density g, the integration over s was truncated at a value of s corresponding to $\tau = 1.7 \times 10^{-5}$ sec. Larger values of τ exceed the dipolar value of T_2 estimated for a rigid methine carbon, and hence the broad lines corresponding to such slow motion will not average with the motionally narrowed lines. It is further noted that Schaefer's eq 26 inadvertently lacks a factor of $(b - 1)^{-1}$, and can be expressed analytically as $g = \bar{\tau}\{[1 - \ln(b)/p]^{-p} - 1\}/(b - 1)$, for $p > \ln(b)$.

Table IV: Comparison of Correlation Times,[a] $\bar{\tau}$, as Derived from T_1, Δ, and NOE Values[b] and the Log–χ^2 Distribution of Correlation Times.[c]

Solvent	$\bar{\tau}(T_1)$	$\bar{\tau}(\Delta)$	$\bar{\tau}$(NOE)
0.15 *M* NaCl–formamide[d]	1	2	2.5
0.15 *M* NaCl–ethanol[e]	1	4	2.5
Dimethyl sulfoxide	1	4	3
0.15 *M* NaCl	120	100	25

[a] In nsec. [b] See Table II. [c] See dashed curves in Figure 1. [d] 5:4, v/v. [e] 1:1, v/v.

Table V: Comparison of $\bar{\tau}$ Values[a] Obtained for *cis*-Polyisoprene and Elastin Using a Log–χ^2 Distribution[b] of Correlation Times having $p = 14$, $b = 1000$ (the volume of solvent absorbed by each elastin sample is also given).

Sample	Solvent	$\bar{\tau}f$	Solvent Absorbed[g]
cis-Polyisoprene[c]	None	0.4	–
Elastin	0.15 *M* NaCl–formamide[d]	1.8	3.0
Elastin	0.15 *M* NaCl–ethanol[e]	2.5	2.5
Elastin	Dimethyl sulfoxide	2.7	4.4
Elastin	0.15 *M* NaCl	80	1.9

[a] In nsec. [b] Defined in eq 1 and 2. [c] Data from Schaefer (1973). [d] 5:4, v/v. [e] 1:1, v/v. [f] For elastin in each solvent $\bar{\tau}$ is the average of the three values given in Table IV; $\tau' = 0.61\,\bar{\tau}$, $\langle\tau\rangle = 13.7\bar{\tau}$, see footnote 1. [g] In ml of solvent per mg of dry native ligamentum nuchae, determined by difference in weights of swollen and dry samples, reproducibility of measurement, ±5%.

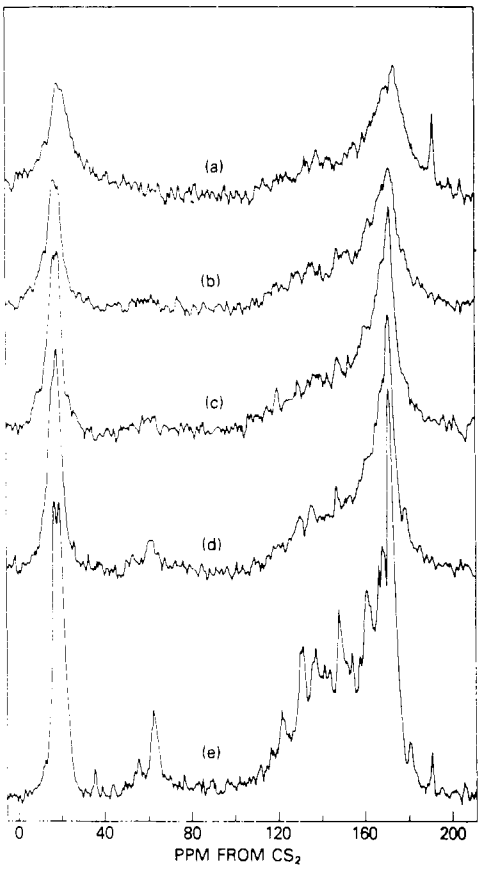

FIGURE 5: Spectra of calf ligamentum nuchae swollen in 0.15 *M* NaCl showing the dependence of line widths on temperature: (a) 24°; (b) 37°; (c) 49°; (d) 55°; (e) 69°. In each case, 8K transients were accumulated using a 90°-t-90° pulse sequence with t = 1.0 sec. Chemical shift scale in ppm from external CS_2. Irreversible spectral changes were caused by significant collagen denaturation above ca. 60°.

discrepancies in the $\bar{\tau}$ values calculated in a single solvent are due in part to the experimental errors in the NMR parameters. However, these discrepancies also arise because exact correlation times cannot be derived using the simple log–χ^2 distribution since this function, at best, approximates the complex distribution of polypeptide segmental motions.[5]

The three calculated values of $\bar{\tau}$ obtained in each solvent (Table IV) were averaged and are compared (Table V) with $\bar{\tau}$ obtained for solid *cis*-polyisoprene (Schaefer, 1973). Due to the long tail of the log–χ^2 distribution, calculated values of $\langle\tau\rangle$ (Table V) are much larger than the corresponding values of $\bar{\tau}$ and τ'.

It is seen (Table V) that, depending upon solvent, $\bar{\tau}$ for swollen elastin is from 4 to 200 times larger than $\bar{\tau}$ for solid *cis*-polyisoprene. The fact that the elastin $\bar{\tau}$ is smallest when the swelling agents contain formamide, the most polar solvent, suggests that differences in $\bar{\tau}$ values among the various solvents are, in part, due to differences in residual polar interactions between the polypeptide chains in the swollen ligament. It is seen (Figure 5e) that at 69° the line widths of ligamentum nuchae, swollen by 0.15 *M* NaCl, are about equal to those obtained at 37° when the ligament is swollen by formamide (Figure 2e) or by 0.15 *M* NaCl-formamide, 5:4, v/v (Figure 3f). Furthermore, in 0.15 *M* NaCl at 69° the backbone carbon NOE value[6] (2.3) is slightly larger than the NOE value (2.0) found in the formamide-containing solvents at 37°. Hence, the chain mobility achieved in 0.15 *M* NaCl is ca. that obtained in the solvents containing formamide, provided that the thermal energy of the chains is 10% greater in the aqueous solvent. The gradual decrease in line width (Figure 5) of elastin swollen in 0.15 *M* NaCl as temperature increases is in accord with the idea that barriers to movement, due to polar interactions, are more rapidly surmounted as thermal energy increases.

Figure 4 provides evidence that interchain polar interactions cannot alone account for the influence of solvent on elastin mobility since it is seen that adding ethanol to 0.15 *M* NaCl decreases line widths. At a solvent composition of 0.15 *M* NaCl-ethanol, 1:1, v/v, $\bar{\tau}$ (Table V) is ca. 30 times less than that found in 0.15 *M* NaCl alone. This result can be explained by assuming that small clusters of hydrophobic side chains aggregate in 0.15 *M* NaCl to reduce contacts with water. When ethanol is added to the aqueous medium, the hydrocarbon portion of the alcohol can shield the side chain from water, thus reducing aggregation and increasing segmental mobility.

The above mentioned hydrophobic and polar interactions

[5] If reorientation is anisotropic, NMR parameters are functions of several (and possibly many) correlation times. In general, the distribution function which determines the contribution of each correlation time to the spectral density will depend upon the orientation of the CH vector with respect to the rotation axes. Hence, the use of a single distribution function for different carbons in the backbone approximately characterizes the *average* chain motion.

[6] The larger NOE, at 69°, and contributions from denatured collagen carbons and all elastin carbons (rather than ca. 80%) are responsible for the 2.5-fold larger intensity observed in Figure 5e as compared with Figure 5b.

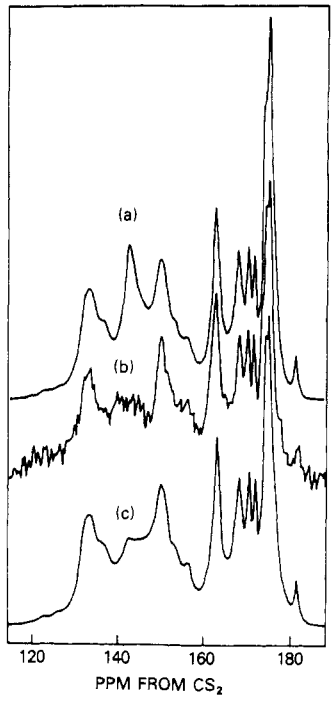

FIGURE 6: Comparison of experimental and calculated upfield spectra of collagen free calf ligamentum nuchae swollen in 0.15 *M* NaCl–formamide, 5:4, v/v; (a) calculated spectrum with all α-carbon Δ/N values equal to 40 Hz; (b) experimental spectrum; (c) calculated spectrum with Ala C^{α} Δ values equal to 150 Hz. In the experimental spectrum 8K transients were accumulated using a 90°-t-90° pulse sequence, t = 1.0 sec, with incoherent proton decoupling gated on only during acquisition (0.25 sec) of the free induction decay. Chemical shift scale in ppm from external CS_2.

must be weak, since the average of $\bar{\tau}$ for elastin swollen in 0.15 *M* NaCl is 80 nsec. Furthermore, the line width and hence $\bar{\tau}$ is significantly reduced on increasing the temperature (Figure 5). This occurs in spite of the fact that the hydrophobic effect would be expected to lead to greater aggregation of hydrophobic groups as temperature increases.[7] Apparently, restrictions on chain motion due to aggregation are more than compensated for by the small increase in the thermal energy.

The dependence of elastin chain mobility on temperature and solvent is in accord with the recent findings of Dorrington et al. (1975). The mechanical measurements of these authors support the network model, and furthermore indicate that the formamide swollen elastin network has the macroscopic dynamical behavior of an ideal rubber-like network, whereas the behavior of the water swollen elastin network is viscoelastic on a time scale of $\lesssim 10^3$ sec. The biological utility of viscoelastic fibrous tissue has been discussed by Dorrington et al. (1975).

Thus far we have discussed elastin chain mobility as if the chain composition were uniform. In fact, the sequence of proelastin shows that there are at least two distinct regions of the polypeptide (Gray et al., 1973). The major portion of the chain consists of repeat sequences of Gly, Pro, and Val residues, whereas the chain composition around the lysine derived cross-links consists almost exclusively of Ala residues. Gray et al. (1973) have proposed an ordered structure (α helix) for the cross-link regions. We have found that a satisfactory simulation of the elastin spectrum in 0.15 *M* NaCl–formamide, 1:1, v/v (Figure 6), is obtained only if Δ/N values for Ala (150 Hz) are about four times those of Gly, Val, and Pro residues (40 Hz). This result does not prove the existence of ordered structure in the cross-link region, but does show that there are significant restrictions on segmental motion in this region. Hence, the reduction of conformational entropy on forming a rigid structure in the cross-link region would be considerably less than elsewhere in the chain. Although one would not expect a hydrogen bond stabilized structure such as an α helix to be stable in solvents containing formamide, such a structure could exist in a less polar solvent such as 0.15 *M* NaCl at 37°.

[7] Hydrocarbon solubility in water decreases as temperature increases (Tanford, 1973) and water swollen ligamentum nuchae shrinks as temperature increases.

Acknowledgments

We thank the Polymers Division of the National Bureau of Standards for the use of their ^{13}C spectrometer, and Mrs. Sheila Taylor for the computer program which was used to calculate the curves in Figure 1. We are grateful to Professor N. G. McCrum for a preprint describing the mechanical studies of elastin carried out by the Oxford group.

References

Abragam, A. (1961), The Principles of Nuclear Magnetism, London, Oxford University Press.

Allerhand, A., Doddrell, D., and Komoroski, R. (1971), *J. Chem. Phys. 55,* 189.

Connor, T. M. (1963), *Trans. Faraday Soc. 60,* 1579.

Doddrell, D., Glushko, V., and Allerhand, A. (1972), *J. Chem. Phys. 56,* 3683.

Dorrington, K., Grut, W., and McCrum, N. G. (1975), *Nature (London)* in press.

Farrar, T. C., Druck, S. J., Shoup, R. R., and Becker, E. D. (1972), *J. Am. Chem. Soc. 94,* 699.

Flory, P. J. (1953), Principles of Polymer Chemistry, Ithaca, N.Y., Cornell University Press.

Gotte, L., Stern, P. M., Elsden, D. F., and Partridge, S. M. (1963), *Biochem. J. 87,* 344.

Gray W. R., Sandberg, L. B., and Foster, J. A. (1973), *Nature (London) 246,* 461.

Grut, W., and McCrum, N. G. (1975), *Nature (London) 251,* 165.

Hoeve, C. A. J., and Flory, P. J. (1958), *J. Am. Chem. Soc. 80,* 6523.

Hoeve, C. A. J., and Flory, P. J. (1974), *Biopolymers 13,* 677.

Hoffman, A. S. (1971), Biomaterials, Bement, Jr., A. L., Ed., Seattle, Wash., University of Washington Press, p 285.

Meyer, K. H., and Ferri, C. (1936), *Pfluegers Arch. Gesamte Physiol. Menschen Tiere 238,* 78.

Mistrali, F., Volpin, D., Garibaldo, G. B., and Ciferri, A. (1971), *J. Phys. Chem. 75,* 142.

Mukherjee, D. P., Hoffman, A. S., and Franzblau, C. (1974), *Biopolymers 13,* 2447.

Oplatka, A., Michaeli, I., and Katchalsky, A. (1960), *J. Polym. Sci. 46,* 365.

Partridge, S. M. (1962), *Adv. Protein Chem. 17,* 227.

Partridge, S. M. (1967), *Nature (London) 213,* 1123.

Partridge, S. M. (1970), in Chemistry and Molecular Biology of the Intercellular Matrix, Vol. 1, Balazs, E. A., Ed., London, Academic Press, p 593.

Partridge, S. M., Davis, H. F., and Adair, G. S. (1955), *Biochem. J. 61,* 11.

Sandberg, L. B., Weissman, N., and Smith, D. W. (1969), *Biochemistry 8,* 2940.
Schaefer, J. (1973), *Macromolecules 6,* 882.
Schaefer, J., and Natusch, D. F. S. (1972), *Macromolecules 5,* 416.
Smith, D. W., Brown, D. M., and Carnes, W. H. (1972), *J. Biol. Chem. 247,* 2427.
Solomon, I. (1955), *Phys. Rev. 99,* 559.
Tanford, C. (1973), The Hydrophobic Effect, New York, N.Y., Wiley.
Thomas, J., Elsden, D. F., and Partridge, S. M. (1963), *Nature (London) 200,* 631.
Treloar, L. R. G. (1958), The Physics of Rubber Elasticity, London, Oxford University Press.
Torchia, D. A., and Lyerla, J. R., Jr. (1974), *Biopolymers 13,* 97.
Torchia, D. A., Lyerla, J. R., Jr., and Quattrone, A. J. (1975), *Biochemistry 14,* 887.
Torchia, D. A., and Piez, K. A. (1973), *J. Mol. Biol. 76,* 419.
Urry, D. W., Mitchell, L. W., and Ohnishi, T. (1974), *Biochemistry 13,* 4083.
Vold, R. L., Waugh, J. S. Klein, M. P., and Phelps, D. E. (1968), *J. Chem. Phys. 47,* 5258.
Weis-Fogh, T., and Andersen, S. O. (1970a), *Nature (London) 227,* 718.
Weis-Fogh, T., and Andersen, S. O. (1970b), in Chemistry and Molecular Biology of the Intercellular Matrix, Vol. 1, Balazs, E. A., Ed., Academic Press, London, p 671.
Woessner, D. E. (1962), *J. Chem. Phys. 37,* 647.
Woessner, D. E., Snowden, B. S., Jr., and Meyer, G. H. (1969), *J. Chem. Phys. 50,* 719.
Wohlisch, E., Weitnauer, H., Gruning, W., and Rohrback, R. (1943), *Kolloid Z. 89,* 239.

The Reconstitution of Microtubules from Purified Calf Brain Tubulin†

James C. Lee and Serge N. Timasheff*

ABSTRACT: The in vitro reconstitution of calf brain tubulin, purified by the method of Weisenberg et al. [(1968), *Biochemistry 7,* 4466–4479; (1970), *Biochemistry 9,* 4110–4116] as modified by Lee et al. [(1973), *J. Biol. Chem. 248,* 7253–7262], was successful in a medium consisting of 10^{-2} *M* sodium phosphate, 10^{-4} *M* GTP, and concentrations of magnesium ions ranging from 0.5 to 16 × 10^{-3} *M* at 37°. Filaments resembling native microtubules were formed. The filaments are in equilibrium with the associating species of tubulin and the equilibrium can be shifted to depolymerization by lowering the temperature to 20°. Filament formation is inhibited by calcium ions which also cause disassembly of the formed filaments. The effects of calcium ion can be reversed by the addition of [ethylenebis(oxyethylenenitrilo)]tetraacetic acid. The formation of filaments is favored by the presence of 3.4 *M* glycerol; only twisted abnormal filaments are observed in the presence of 1 *M* sucrose. The high molecular weight components observed in the sodium dodecyl sulfate polyacrylamide gel electrophoresis patterns of many tubulin preparations were shown not to be essential for the formation of the filaments.

The initial description by Weisenberg (1972) of the reconstitution of microtubules from partially purified brain tubulin has been followed by a number of reports on this system (Borisy and Olmsted, 1972; Shelanski et al., 1973; Kirschner et al., 1974; Erickson, 1974). In all of these studies, the starting material was either partially purified protein or crude homogenate of brain protein. No studies on the reconstitution of microtubules from tubulin purified by the Weisenberg (Weisenberg et al., 1968; Weisenberg and Timasheff, 1970) procedure have been described, although the statement has been made in the literature that "the colchicine binding protein isolated by this method does not polymerize into microtubules" (Weingarten et al., 1974). The demonstration by Frigon et al. (Frigon et al., 1974; Frigon and Timasheff, 1975a,b) that calf brain tubulin purified by the Weisenberg procedure could undergo a self-association reaction in the presence of magnesium ions with the formation of closed ring polymers with a most probable molecular weight of 2.86 × 10^6 prompted us to investigate whether even larger, possibly filamentous, aggregates could be induced to form from the pure fully dissociated protein. A preliminary electron microscopic study having indicated that microtubules can indeed be reconstituted from highly purified calf brain tubulin (Lee et al., 1975a,b), a detailed study of the reassembly of tubulin was initiated and the results are reported in this paper.

Materials and Methods

Sodium dodecyl sulfate, purchased from Fisher Scientific Co., was recrystallized before use. Acrylamide was obtained from Bio-Rad Laboratories. Spectroquality glycerol was purchased from Matheson Coleman and Bell, and ultra pure sucrose (lot ZZ 1604) was from Schwarz/Mann. Uranyl acetate and [ethylenebis(oxyethylenenitrilo)]tetraacetic

† Publication 1048 of the Graduate Department of Biochemistry, Brandeis University, Waltham, Massachusetts 02154. *Received June 18, 1975.* Supported by National Institutes of Health Grants GM-14603 and CA 16707, National Science Foundation Grant GB-38544X, and a grant from the American Cancer Society, Massachusetts Division.